



**This is an Open Access-journal's PDF published in**

**Bernardo-García, N., Bartual, S.G., Fulde, M., Bergmann, S.,  
Hermoso, J.A.**

**Crystallization and preliminary X-ray diffraction analysis of  
phosphoglycerate kinase from *Streptococcus pneumoniae***

**(2011) Acta Crystallographica Section F: Structural Biology and  
Crystallization Communications, 67 (10), pp. 1285-1289**

**Noelia Bernardo-García,<sup>a</sup>  
 Sergio G. Bartual,<sup>a</sup> Marcus  
 Fulde,<sup>b</sup> Simone Bergmann<sup>b,c</sup> and  
 Juan A. Hermoso<sup>a\*</sup>**

<sup>a</sup>Department of Crystallography and Structural Biology, Instituto de Química-Física 'Rocasolano', CSIC, Serrano 119, 28006 Madrid, Spain, <sup>b</sup>Department of Medical Microbiology, Helmholtz Centre of Infection Research, Inhoffenstrasse 7, 38124 Braunschweig, Germany, and <sup>c</sup>Department of Infection Biology, Institute for Microbiology, Technische Universität Braunschweig, Spielmannstrasse 7, 38106 Braunschweig, Germany

Correspondence e-mail: xjuan@iqfr.csic.es

Received 26 May 2011

Accepted 1 August 2011

## Crystallization and preliminary X-ray diffraction analysis of phosphoglycerate kinase from *Streptococcus pneumoniae*

Phosphoglycerate kinase (PGK) is a widespread two-domain enzyme that plays a critical role in the glycolytic pathway. Several glycolytic enzymes from streptococci have been identified as surface-exposed proteins that are involved in streptococcal virulence by their ability to bind host proteins. This binding allows pneumococcal cells to disseminate through the epithelial and endothelial layers. Crystallization of PGK from *Streptococcus pneumoniae* yielded orthorhombic crystals (space group *I*222, unit-cell parameters  $a = 62.73$ ,  $b = 75.38$ ,  $c = 83.63$  Å). However, the unit cell of these crystals was not compatible with the presence of full-length PGK. Various analytical methods showed that only the N-terminal domain of PGK was present in the *I*222 crystals. The ternary complex of PGK with adenylyl imidodiphosphate (AMP-PNP) and 3-phospho-D-glycerate (3PGA) produced monoclinic crystals (space group *P*2<sub>1</sub>, unit-cell parameters  $a = 40.35$ ,  $b = 78.23$ ,  $c = 59.03$  Å,  $\beta = 96.34^\circ$ ). Molecular replacement showed that this new crystal form contained full-length PGK, thereby indicating the relevance of including substrates in order to avoid proteolysis during the crystallization process.

### 1. Introduction

*Streptococcus pneumoniae* is a major cause of life-threatening infections such as pneumonia, meningitis and septicaemia worldwide. Successful infection depends on pathogen–host interaction and it is thought that surface-exposed proteins are critical to this relationship by providing the first contact of the pathogen with its intended host (Bergmann & Hammerschmidt, 2006; Hammerschmidt, 2006). Recently, it has been shown that streptococcal phosphoglycerate kinase (PGK), a member of the glycolytic proteins, is a surface-exposed protein. Proteomic analyses of *S. agalactiae* have revealed the presence of PGK, enolase and glyceraldehyde-3-phosphodehydrogenase (GAPDH) on the surface of these group B streptococci (Hughes *et al.*, 2002). However, the mechanisms of cell-wall binding and secretion for these glycolytic proteins remain unknown (Bergmann *et al.*, 2003). Glycolytic enzymes of streptococci have been identified as multifunctional virulence factors, mediating interaction with host components involved in haemostasis and in bacterial binding to extracellular matrix proteins (Bergmann & Hammerschmidt, 2006; Pancholi *et al.*, 2003). One example is GAPDH of group A streptococci, which is directly involved in streptococcal adherence and colonization (Jin *et al.*, 2005), in circumventing the host immune defence (Terao *et al.*, 2006) and, together with pneumococcal enolase, in mediating the degradation of extracellular matrix proteins (Bergmann *et al.*, 2005; Hammerschmidt, 2006). *S. pneumoniae* PGK (41.9 kDa) is a major component of the glycolytic pathway, facilitating the transfer of the anhydride phosphate of 1,3-bisphospho-D-glycerate (1,3-BPG) to adenosine 5'-diphosphate magnesium salt (MgADP), yielding 3-phospho-D-glycerate (3PGA) and adenosine 5'-triphosphate magnesium salt (MgATP) (Bernstein *et al.*, 1997). PGK is monomeric and folds into two globular domains (Pecorari *et al.*, 1996). The N-terminal domain binds 3PGA and the C-terminal



© 2011 International Union of Crystallography  
 All rights reserved

domain binds MgADP; a linker is retained between the two domains that is susceptible to attack by proteases.

Here, we describe the preliminary crystallographic results obtained for the N-terminal domain of PGK (N-PGK) and for full-length PGK as a ternary complex with 3PGA and AMP-PNP.

## 2. Experimental procedures

### 2.1. Expression and purification of PGK

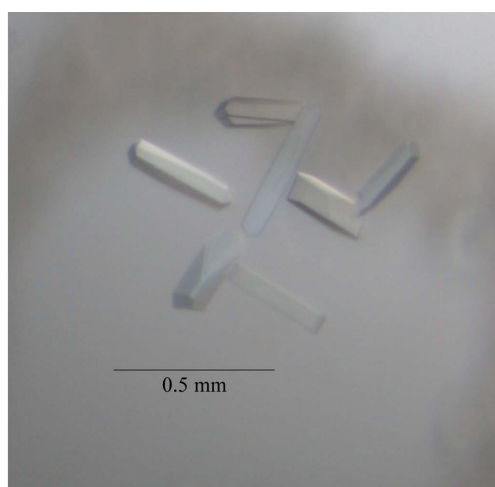
A DNA fragment comprising the full-length protein (YP\_815953.1) was amplified by PCR using the oligonucleotides left primer (5'-GGGGATCCTTGGCAAACTACTGTAAAGAG-3') and right primer (5'-CCCGTCGACTTATTTTCTGTCAAGGC-TGCAAG-3'). The sequences in bold indicate restriction-site linkers (*Bam*HI and *Sal*I, respectively) in the pQE30 plasmid (Qiagen,

Düsseldorf, Germany), yielding pQE30PGKw. A six-histidine tag was included at the N-terminus of the construct. A 5 ml aliquot of *Escherichia coli* strain M15 (pREP) freshly transformed with pQE30PGKw was used as a starter inoculum in 250 ml LB medium supplemented with 100 µg ml<sup>-1</sup> ampicillin and 50 µg ml<sup>-1</sup> kanamycin. It was then incubated with vigorous shaking overnight at 309 K. After supplementation with 250 ml LB medium without antibiotics, protein expression was induced by the addition of 1 mM IPTG and growth was continued for 4 h at 301 K. Bacterial cultures were sedimented by centrifugation at 2980g for 20 min. The supernatant was discarded and the pellet was dissolved in 10 ml phosphate-buffered saline (50 mM NaH<sub>2</sub>PO<sub>4</sub>, 300 mM NaCl adjusted to pH 8.0) supplemented with 1 mM PMSF to reduce nonspecific protease cleavage. Mechanical lysis was performed using a French pressure cell (SLM-Aminco). Lysates were centrifuged for 30 min at 17 211g and the supernatant was loaded onto a Ni-NTA column (Qiagen) for purification of the His-tagged protein at room temperature. The Ni-NTA column was washed with 20 mM imidazole in sodium phosphate-buffered saline (50 mM NaH<sub>2</sub>PO<sub>4</sub>, 300 mM NaCl adjusted to pH 8.0) to remove nonspecific protein debris and the recombinant protein was eluted with 250 mM imidazole in the same buffer.

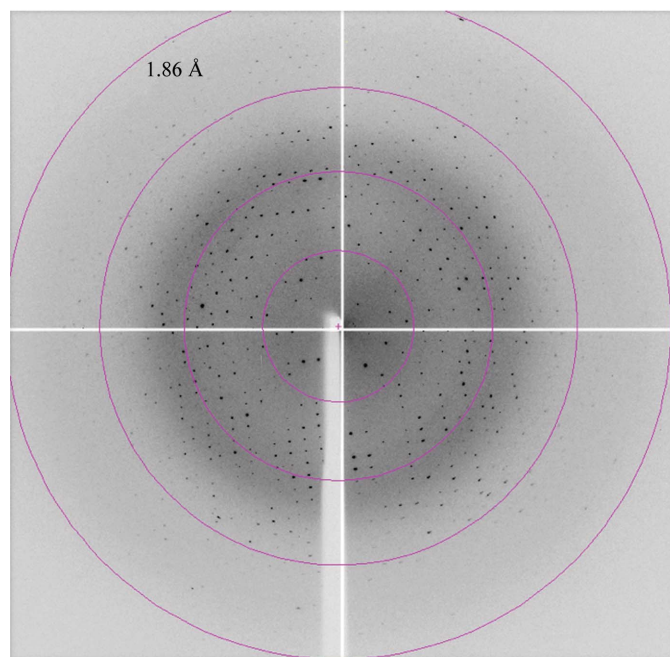
The protein solution was dialysed in a dialysis tube with a molecular-weight cutoff of 12–14 kDa millipore against phosphate-buffered saline (50 mM NaH<sub>2</sub>PO<sub>4</sub>, 300 mM NaCl adjusted to pH 8.0) at 277 K to remove the imidazole. Protein concentration was measured by absorbance at 280 nm (NanoDrop spectrophotometer) and by the Bradford assay (Bio-Rad, Hertfordshire, UK). Expression quality was checked by SDS-PAGE.

### 2.2. Mass spectrometry: molecular-weight determination

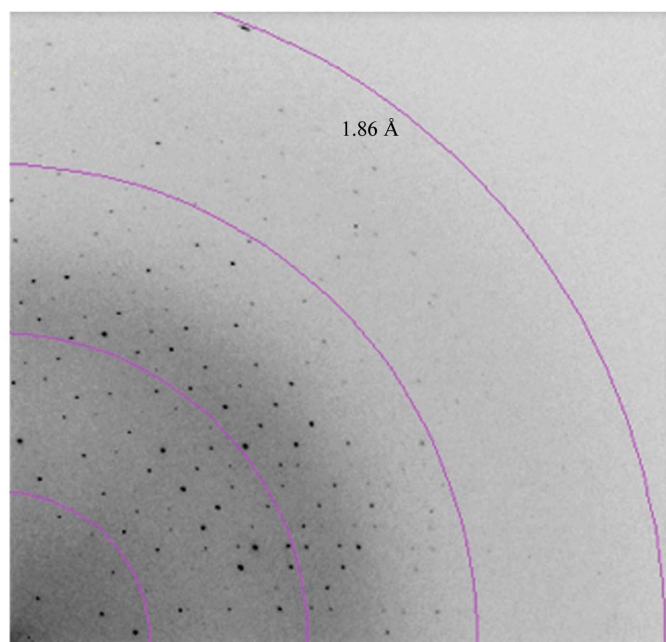
Mass spectra were acquired using an ABI 4800 MALDI-TOF/TOF analyzer (Applied Biosystems, Framingham, Massachusetts, USA) in linear mode with an Nd:YAG 355 nm wavelength laser, averaging 1000 laser shots.



(a)



(b)



(c)

**Figure 1**

(a) The best N-PGK crystals were grown using the hanging-drop vapour-diffusion method and a reservoir solution consisting of 32% (w/v) polyethylene glycol 4000 in 0.1 M Tris-HCl pH 7.5 and 0.2 M Li<sub>2</sub>SO<sub>4</sub>. (b) Diffraction image of an N-PGK crystal diffracting to 1.86 Å resolution (1.0° oscillation range). (c) Enlargement showing the highest resolution area.

### 2.3. MALDI peptide mass fingerprinting (PMF) and tandem mass spectrometry (MS/MS)

For MALDI-TOF/TOF analysis, data were automatically acquired using an ABI 4800 MALDI-TOF/TOF mass spectrometer (Applied Biosystems, Framingham, Massachusetts, USA) in positive-ion reflector mode (the ion-acceleration voltage was 25 kV for MS acquisition and 1 kV for MS/MS) and the obtained spectra were stored in the ABI 4000 Series Explorer Spot Set Manager. PMF and MS/MS fragment-ion spectra were smoothed and corrected to zero baseline using routines embedded in *ABi 4000 Series Explorer v.3.6* software. Each PMF spectrum was internally calibrated with the mass signals of trypsin-autolysis ions to reach a typical mass measurement accuracy of <25 p.p.m. Known trypsin and keratin mass signals, as well as potential sodium and potassium adducts (+21 and +39 Da), were removed from the peak list. *GPS Explorer v.4.9* was used to submit the combined PMF and MS/MS data to *MASCOT* software v.2.2.04 (Matrix Science, London, England) by searching in the nonredundant NCBI protein database.

### 2.4. Crystallization

Extensive assays to identify crystallization conditions for PGK were carried out by the sitting-drop vapour-diffusion method at 291 K using Innovaplate SD-2 microplates (Innovadyne Technologies Inc., California, USA). The His tag was retained on the protein during crystallization trials. The initial crystallization screening kits were Crystal Screen HT, Index HT (Hampton Research, Aliso Viejo, California, USA), JCSG+ Suite and PACT Suite (Qiagen, Düsseldorf, Germany). 500 nl droplets were prepared by mixing 250 nl reservoir solution with 250 nl protein solution at a concentration of 5 mg ml<sup>-1</sup> in phosphate-buffered saline (50 mM NaH<sub>2</sub>PO<sub>4</sub>, 300 mM NaCl adjusted to pH 8.0) with a NanoDrop robot (Innovadyne Technologies Inc.). The droplets were equilibrated against 65 µl reservoir solution. For the cocrystallization trials, the protein solution was prepared as follows. 50 µl protein solution (6 mg ml<sup>-1</sup> in 50 mM NaH<sub>2</sub>PO<sub>4</sub>, 300 mM NaCl adjusted to pH 8.0) was mixed with 5 µl of each of the substrates: 100 mM AMP-PNP (adenylyl imidodiphos-

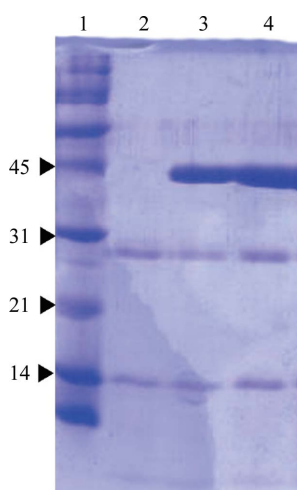


**Figure 2** SDS-PAGE analysis of dissolved PGK crystals. Lane 1, standard broad-range (Bio-Rad) molecular-weight markers (labelled in kDa). Lane 2, dissolved PGK crystals (N-PGK) belonging to space group *I222*; the crystals presented a band of approximately 25 kDa. Lanes 3 and 4, samples of the PGK protein solution stored at 193.15 K for three months. The band at 41.9 kDa corresponds to the full-length protein and the band at 25 kDa corresponds to the N-terminal domain of PGK. A third band is also observed at 14 kDa, which could be related to degradation of the C-terminal domain. Coomassie Blue staining was used for protein detection.

**Table 1**

Data-collection statistics for N-PGK and the ternary complex PGK-AMP-PNP-3PGA.

Values in parentheses are for the highest resolution shell.

	N-terminal PGK domain (N-PGK)	PGK-AMP-PNP-3PGA ternary complex
Crystal data		
Space group	<i>I222</i>	<i>P2<sub>1</sub></i>
Unit-cell parameters		
<i>a</i> (Å)	62.76	40.35
<i>b</i> (Å)	75.38	78.23
<i>c</i> (Å)	83.63	59.03
$\alpha$ (°)	90	90
$\beta$ (°)	90	96.34
$\gamma$ (°)	90	90
Data collection		
Temperature (K)	100	100
Radiation source	ESRF beamline ID14-1	ESRF beamline ID14-2
Detector	ADSC Quantum Q315r detector	ADSC 210 CCD detector
Wavelength (Å)	0.933	0.934
Resolution range (Å)	31.59–2.08 (2.11–2.08)	46.94–1.78 (1.88–1.78)
No. of images	180	180
Measured reflections	82242	129733
Unique data	12253	34968
Multiplicity	6.7 (6.8)	3.7 (3.6)
Data completeness (%)	100 (100)	99.9 (100)
Average $I/\sigma(I)$	29.4 (4.2)	27.5 (2.2)
$R_{\text{merge}}^{\dagger}$	0.10 (0.42)	0.08 (0.59)

<sup>†</sup>  $R_{\text{merge}}$  is defined as  $\sum_{hkl} \sum_i |I_i(hkl) - \langle I(hkl) \rangle| / \sum_{hkl} \sum_i I_i(hkl)$ , where  $I_i(hkl)$  is the intensity of an individual reflection and  $\langle I(hkl) \rangle$  is the average intensity for this reflection; the summation is over all intensities.

phate, an ATP analogue) and 100 mM 3PGA (3-phospho-D-glycerate). All samples were incubated for 1 h on ice with Complete EDTA-free protease inhibitor (Roche Applied Science) just before crystallization assays.

Positive results were scaled up using the hanging-drop vapour-diffusion method in Linbro plates (Hampton Research), mixing 1 µl protein solution with 1 µl reservoir solution and equilibrating the drops against 0.5 ml crystallization solution in the reservoir.

### 2.5. X-ray data collection and processing

X-ray diffraction data sets were collected at 100 K using an ADSC (Area Detector Systems Corporation) Quantum Q315r detector on beamline ID 14-1 ( $\lambda = 0.934$  Å) or an ADSC 210 CCD detector on beamline ID 14-2 ( $\lambda = 0.933$  Å) at the ESRF, Grenoble, France. Cryoprotection of the crystals for data collection was achieved by transferring them for a few seconds into a solution consisting of 15% (v/v) glycerol in the optimized reservoir solution, followed by flash-cooling in liquid nitrogen. Collected data were processed using *iMOSFLM* (Battye *et al.*, 2011) and scaled with *SCALA* (Winn *et al.*, 2011).

### 2.6. Preliminary structure solution

PGK structure determination was initiated using the *Thermotoga maritima* PGK structure (PDB entry 1vpe; Auerbach *et al.*, 1997), which shows 55.4% sequence identity to pneumococcal PGK. This model was used as a template in the molecular-replacement method using *MOLREP* (Vagin & Teplyakov, 2010).

## 3. Results

PGK crystals grew within 1 d from 30% (w/v) polyethylene glycol (PEG) 4000, 200 mM Li<sub>2</sub>SO<sub>4</sub> and 100 mM Tris-HCl pH 8.5 (condition No. 17 of Crystal Screen HT; Hampton Research). Optimization of

crystal quality was achieved by testing different pH values and by lowering the PEG concentration.

The largest PGK crystals, with maximum dimensions of about  $0.5 \times 0.25 \times 0.5$  mm, were obtained after optimization by the hanging-drop vapour-diffusion method against a reservoir solution consisting of 32% (w/v) PEG 4000, 200 mM  $\text{Li}_2\text{SO}_4$  and 100 mM Tris-HCl pH 7.5. (Fig. 1a).

An X-ray data set was collected to 2.0 Å resolution from a PGK crystal and showed a well defined diffraction pattern (Fig. 1b). The crystals belonged to the orthogonal space group  $I222$ , with unit-cell parameters  $a = 62.76$ ,  $b = 75.38$ ,  $c = 83.63$  Å. Specific volume calculations based on the molecular weight of full-length PGK (Matthews, 1968) indicated that the asymmetric unit could not even contain one PGK molecule (solvent content of 4.34% and  $V_M = 1.18 \text{ Å}^3 \text{ Da}^{-1}$ ).

The obtained solvent content was obviously not compatible with the presence of full-length PGK in the crystals.

In order to understand this result, we decided to carry out SDS-PAGE analysis, a mass-spectrometric assay and fingerprinting of the PGK crystals. The SDS-PAGE analysis (Fig. 2) indicated that the protein in the crystal was proteolyzed, presenting a molecular mass of 25 kDa instead of the 41.9 kDa expected for the full-length protein. Mass spectrometry confirmed these results. Fingerprinting of the PGK crystals indicated the presence of only the N-terminal domain of PGK (N-PGK) in the crystals (220 amino acids). The Matthews coefficient was recalculated assuming one N-PGK molecule per asymmetric unit, yielding a  $V_M$  of  $2.39 \text{ Å}^3 \text{ Da}^{-1}$  and a solvent content of 48.63%.

In order to gain stability and avoid proteolysis of the full-length PGK, crystallization in the presence of AMP-PNP and 3PGA was attempted. Crystals of the ternary PGK-AMP-PNP-3PGA complex grew from a reservoir solution consisting of 30% (w/v) PEG 4000, 0.2 M  $\text{MgCl}_2$  and 0.1 M Tris-HCl pH 8.6. Drops were prepared by mixing 2 µl of this reservoir solution with 4 µl protein solution ( $5 \text{ mg ml}^{-1}$  in the same buffer as previously) and including 0.5 µl 25 mM *n*-decanoyl sucrose as an additive (Fig. 3a). Crystals of the ternary PGK-AMP-PNP-3PGA complex presented a different habit to that of the native crystals. The ternary complex crystals grew to maximum dimensions of  $0.25 \times 0.10 \times 0.25$  mm within 3 d at a temperature of 291.15 K. An X-ray data set for the ternary PGK-AMP-PNP-3PGA complex was collected to 1.78 Å resolution and displayed a well defined diffraction pattern (Fig. 3b). X-ray diffraction data were processed and showed good data-collection statistics (Table 1). These crystals belonged to the monoclinic space group  $P2_1$ , with unit-cell parameters  $a = 40.35$ ,  $b = 78.23$ ,  $c = 59.03$  Å,  $\beta = 96.35^\circ$ . Specific volume calculations based on the molecular mass of full-length PGK (398 amino acids, 41 953 Da) indicated the probable

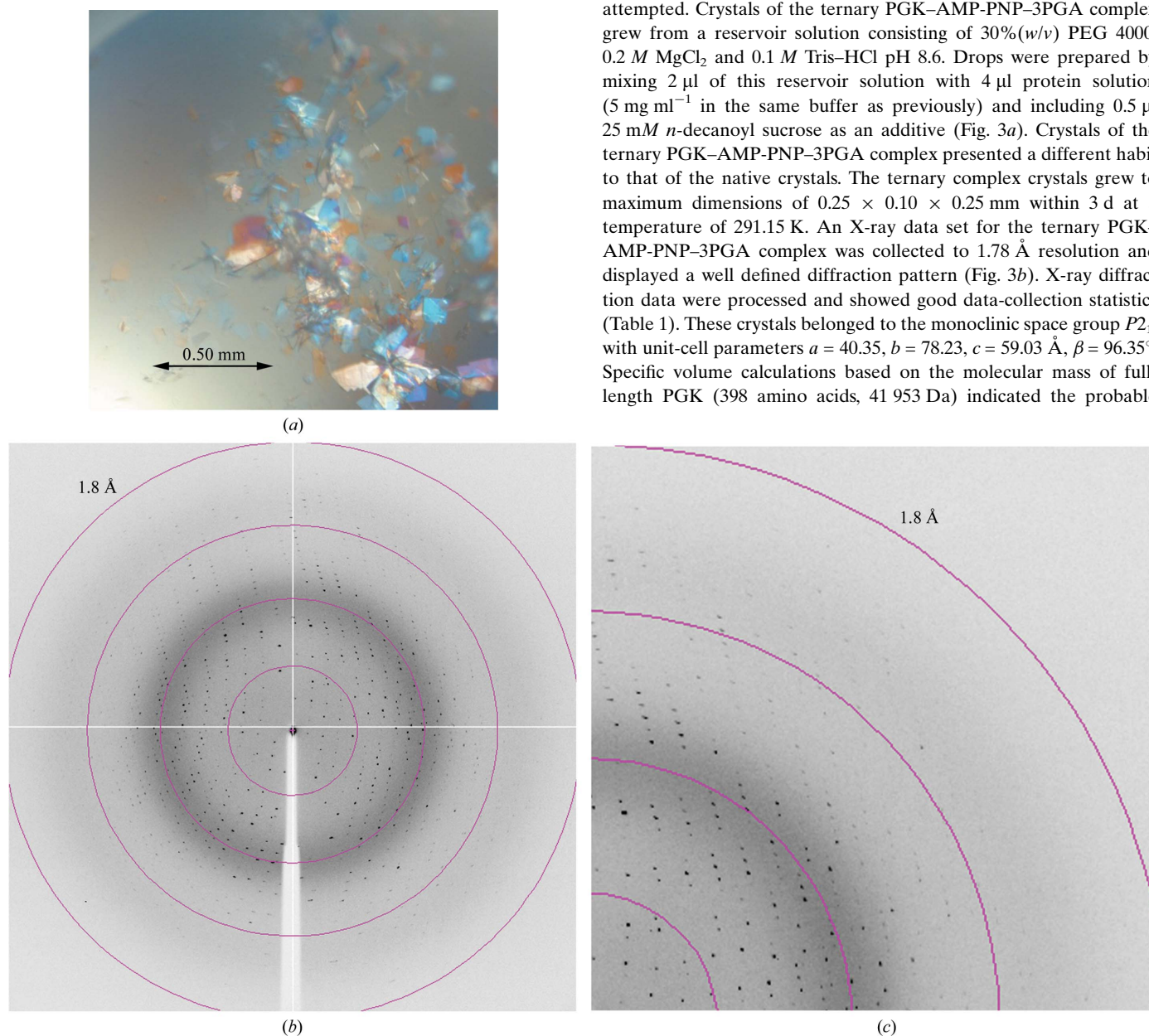


**Figure 3** (a) Crystals of the PGK-AMP-PNP-3PGA ternary complex were obtained using the hanging-drop vapour-diffusion method and a reservoir solution consisting of 30% (w/v) polyethylene glycol 4000, 0.2 M  $\text{MgCl}_2$  and 0.1 M Tris-HCl pH 8.6. The drops were prepared by mixing 2 µl reservoir solution with 4 µl protein solution ( $5 \text{ mg ml}^{-1}$ ) and including 0.5 µl 25 mM *n*-decanoyl sucrose as an additive. (b) Diffraction image of a PGK-AMP-PNP-3PGA crystal diffracting to 1.78 Å resolution ( $1.0^\circ$  oscillation range). (c) Enlargement showing the highest resolution area.

presence of one PGK molecule per asymmetric unit, with 44.27% solvent content and a Matthews coefficient  $V_M$  of  $2.21 \text{ \AA}^3 \text{ Da}^{-1}$ . Molecular replacement further confirmed the presence of full-length PGK protein in the crystals of the ternary complex. These results revealed that the presence of AMP-PNP and 3PGA prevented the proteolysis observed for the N-PGK crystals. Structural refinement of the ternary PGK–AMP–PNP–3PGA complex is currently in progress.

## References

- Auerbach, G., Huber, R., Grättinger, M., Zaiss, K., Schurig, H., Jaenicke, R. & Jacob, U. (1997). *Structure*, **5**, 1475–1483.
- Battye, T. G. G., Kontogiannis, L., Johnson, O., Powell, H. R. & Leslie, A. G. W. (2011). *Acta Cryst.* **D67**, 271–281.
- Bergmann, S. & Hammerschmidt, S. (2006). *Microbiology*, **152**, 295–303.
- Bergmann, S., Rohde, M., Preissner, K. T. & Hammerschmidt, S. (2005). *Thromb. Haemost.* **94**, 304–311.
- Bergmann, S., Wild, D., Diekmann, O., Frank, R., Bracht, D., Chhatwal, G. S. & Hammerschmidt, S. (2003). *Mol. Microbiol.* **49**, 411–423.
- Bernstein, B. E., Michels, P. A. & Hol, W. G. (1997). *Nature (London)*, **385**, 275–278.
- Hammerschmidt, S. (2006). *Curr. Opin. Microbiol.* **9**, 12–20.
- Hughes, M. J. *et al.* (2002). *Infect. Immun.* **70**, 1254–1259.
- Jin, H., Song, Y. P., Boel, G., Kochar, J. & Pancholi, V. (2005). *J. Mol. Biol.* **350**, 27–41.
- Matthews, B. W. (1968). *J. Mol. Biol.* **33**, 491–497.
- Pancholi, V., Fontan, P. & Jin, H. (2003). *Microb. Pathog.* **35**, 293–303.
- Pecorari, F., Guilbert, C., Minard, P., Desmadril, M. & Yon, J. M. (1996). *Biochemistry*, **35**, 3465–3476.
- Terao, Y., Yamaguchi, M., Hamada, S. & Kawabata, S. (2006). *J. Biol. Chem.* **281**, 14215–14223.
- Vagin, A. & Teplyakov, A. (2010). *Acta Cryst.* **D66**, 22–25.
- Winn, M. D. *et al.* (2011). *Acta Cryst.* **D67**, 235–242.